Available online at www.sciencedirect.com

SciVerse ScienceDirect

Ceramics International 38 (2012) 4277–4283

CERAMICS INTERNATIONAL

www.elsevier.com/locate/ceramint

Patterned Zn-seeds and selective growth of ZnO nanowire arrays on transparent conductive substrate and their field emission characteristics

C.M. Yang [a], M.H. Hon [a], I.C. Leu [b,*]

[a] Department of Materials Science and Engineering, National Cheng Kung University, Tainan 701, Taiwan, ROC
[b] Department of Materials Science, National University of Tainan, Tainan 700, Taiwan, ROC

Received 3 January 2012
Available online 9 February 2012

Abstract

A method for the patterned growth of ZnO nanorods with better field emission properties is presented that combines nanoimprinting, electroplated Zn seeds and aqueous solution growth of ZnO. A patterned Zn layer over large area was prepared using the poly(dimethylsiloxane) (PDMS) template to pattern PMMA masking layer without residual layer. ZnO nanorods were selectively deposited on the Zn seeds instead of growing on the bare ITO regions due to the preferred growth on Zn seeds/ITO substrate. The diameter of ZnO nanorods was decided by the concentration of reactants of zinc nitrate and hexamethyltetramine ($C_6H_{12}N_4$) (0.025–0.1 M) at low temperature. This approach provides the capability of creating patterned 1D ZnO micro/nanopatterns at low temperature, ambient condition, and low cost with large area on flexible devices.

Keywords: D. ZnO; Field emission (FE); Transparent conductive substrate; Selective growth

1. Introduction

Field emission (FE) of zinc oxide (ZnO) nanostructures has received a great attention due to its potential applications in vacuum microelectronic devices such as field emission displays, X-ray sources, microwave devices, etc. Zinc oxide, a wide band gap (E_g = 3.37 eV) semiconductor with a large exciton binding energy (60 meV) is important in electronic applications. ZnO is a typical n-type wide band gap semiconductor, playing an important role in many fields ranging from optoelectronics to energy conversion, photocatalysis, photodectors, and nanosensors [1–7]. One-dimensional (1D) nanostructures have been intensively studied in the past years owing to their special properties and potential applications in nanoscale electric and optoelectronic devices. An important issue in this field is how to realize the controllable growth of 1D nanostructures to obtain the desired functionality. For the applications in nanodevices, it is necessary to control the density and the exact growing positions of the ZnO nanorods on the substrate. In other words, instead of randomly placing nanorods on a substrate a more effective method is to selectively grow nanostructures directly onto electrodes or other desirable areas of the substrate. Generally, the technique utilized to achieve a site-specific growth of ZnO nanorods or nanowires involves patterning and selective growth. In conventional patterning of ceramic thin films, the processing window is narrow and it is hard to find suitable etching conditions to obtain patterned ZnO nanorods [8]. To solve this problem, selective growth techniques is a more direct, effective and feasible method. Besides, using this technique, ZnO nanorod arrays with tunable spacing and diameter are achieved, which also have uniform shape and length, and good crystal quality aligned on the ITO substrates. For example, patterning ZnO nanorod arrays defined by polystyrene (PS) microsphere [9] [10], preparation of ZnO micropatterns using self-assembled monolayer [8] [11]; and determining growth positions of ZnO nanorod arrays via coating the ZnO–C seed layer with patterned photoresist prepared by conventional photolithography [12], have been reported in the literature. However, these approaches are limited by high temperature treatment, expensive substrate, high vacuum system, lithography or complication of process details. Thus, a new micro/nanopatterning technique conducted

* Corresponding author. Present address: 33, Sec. 2, Su-Lin St., Tainan 700, Taiwan, ROC. Tel.: +886 6 2380208; fax: +886 6 2380208.
E-mail address: icleu@mail.mse.ncku.edu.tw (I.C. Leu).

0272-8842/$36.00
doi:10.1016/j.ceramint.2012.01.085

at low temperature is desirable. In this paper, the whole process, starting from nanoimprint lithography (NIL) patterning of electroplated seeds to guide the growth of nanorods, is thus environment friendly, quick and feasible.

In this work, we electroplated Zn seeds and used the aqueous solution growth method to grow ZnO NRs on indium tin oxide (ITO) substrate. The patterned zinc seeds were transformed into oxidized zinc species cluster in precursor solution before the aqueous solution method growth stage. These oxidized zinc species cluster provide a lattice-matched buffer layer for further growth of oriented ZnO NRs in aqueous solution process. Thus, selective growth of ZnO using a micro/nanopatterning technique at low temperature and aqueous solution method is applicable to transparent electrodes and the use of ZnO nanorods in integrated device technology is greatly anticipated [8].

2. Experimental details

The ITO/glass and ITO/PET substrates with a sheet resistance of 15 and 50 Ω square^{-1} were employed, respectively. The ITO glass substrates used in our studies were ultrasonic bath cleaned by acetone, isopropyl alcohol (IPA) and deionized (DI) water each for 20 min, followed by N_2 gas drying, immediately prior to use. The PDMS mold was fabricated by spin-coating a 10:1 ratio mixture of Sylgard 184 (from Dow Corning) and curing agent on the anti-adhesion-treated Si master mold, which has nano-dot and line array patterns with a pitch of 550 nm and 830 nm, respectively. These soft molds were cured for 1 h at room temperature and then for 4 h at 60 °C in the oven. Then the patterned PDMS molds were immersed in the alcohol (95%) for 5 min before proceeding to imprinting process. The resist material of poly-(methyl methacrylate) (PMMA) (70,000 average molecular weight) was dissolved in chlorobenzene, and was then spin coated on the ITO substrate with the first step at 500 rpm for 10 s and followed by the second step at 3000 rpm for 30 s at the thickness of about 60 nm. And these films were heated at 60 °C for 20 min on hot plate, in order to remove the organic solvent. The elastic PDMS mold was pressed on to the PMMA film with a small applied pressure of 0.01 MPa at 60 °C for 20 min. After cooling to room temperature, the patterns of PMMA on ITO substrate were obtained by removing the PDMS mold.

Those patterned ITO substrates were electroplated with Zn seeds on the exposed area of the ITO film. The electroplating process was carried out in a three-electrode system, in which Pt worked as the counter electrode, an Ag/AgCl (in saturated NaCl) served as the reference electrode and the ITO substrate was used as the working electrode. The zinc plating solution contained 0.56 M $ZnSO_4{\cdot}7H_2O$, 0.63 M Na_2SO_4, 0.51 M NaCl and 0.32 M H_3BO_3 dissolved in deionized water. The bath temperature was kept at room temperature. After applying a current of 5 mA/cm^2 for 1 min, patterned Zn seeds were obtained. These samples were rinsed with DI water and N_2 gas drying immediately. Electrochemical experiments were carried out with an EG&G Princeton Applied Research model 273A potentiostat/galvanostat.

The zinc oxide nanorods were grown on patterned substrates by the aqueous chemical growth method. Solutions of equal molar concentration of zinc nitrate hexahydrate ($Zn(NO_3)_2{\cdot}6H_2O$) and hexamethyleneteramine ($C_6H_{12}N_4$) were mixed. The concentrations of reaction solution were 0.025 and 0.1 M, respectively. The mixed solution was stirred at room temperature for 10 min for well mixing and the deposition was performed at 90 °C. The side with the seed layer was adhered facing down in the solution. The concentrations were 0.025 and 0.1 M, respectively. And a deposition time of 3 h was used to obtain the ZnO nanorod arrays. After the growth was completed, the samples were cleaned by DI water and N_2 gas drying immediately. As reported in the literature, the following reactions are believed to take place in the formation of ZnO nanorods [13].

$$(CH_2)_6N_4 + 6H_2O \rightarrow 6HCHO + 4NH_3$$

$$NH_3 + H_2O \rightarrow NH_4^+ + OH^-$$

$$2OH^- + Zn^{2+} \rightarrow Zn(OH)_2$$

$$Zn(OH)_2 \xrightarrow{\Delta} ZnO_{(s)} + H_2O$$

The morphologies and structures of the deposited materials were investigated by scanning electron microscopy (SEM) using a Hitachi S4200 field-emission SEM, and X-ray diffractometry (XRD) using a Rigaku D/max X-ray diffractometer, respectively.

3. Result and discussion

Zn and ZnO crystals have identical hexagonal structures and relatively small lattice mismatches of 4.9% and 18.0% along the *c*- and *a*-axes, respectively. ZnO NRs thus tend to grow epitaxially and well-aligned on seeded substrates [14] [15]. The same growth conditions on ITO substrates without seeds will produce sparse, random and large-diameter ZnO NRs. A patterned Zn film is used to initiate and define regions of nanostructure growth. The size and morphology of Zn seed layers are greatly affected by the experimental parameters, such as temperature, voltage, current density and reaction time during seed electroplating. The nanoimprinting is performed to pattern PMMA on ITO substrate. Since the nanoimprint process can be tuned to be residual layer-free, electroplating of Zn patterns can take place on the ITO substrate outside the PMMA masking. Figs. 1–3 give examples of the micro/nanopatterns of Zn seeds defined by the patterned PMMA under different electroplating conditions. All of them demonstrate good selectivity achieved using such an electroplating process. In Fig. 1(a), the linear Zn seeds are distinct from Fig. 1(b), if the current density is increased further to 20 mA/cm^2 (as Fig. 1(a)), the growth of Zn lined pattern will be more irregular. The phenomenon is caused by the high transient current to deposit larger Zn grain, and the resulted in uneven edge of the lines. Fig. 1 shows the difference between (c) and (d) is grain size, the larger current density induces the larger grains. On the contrary, the smaller current density will get the smaller grains. When the

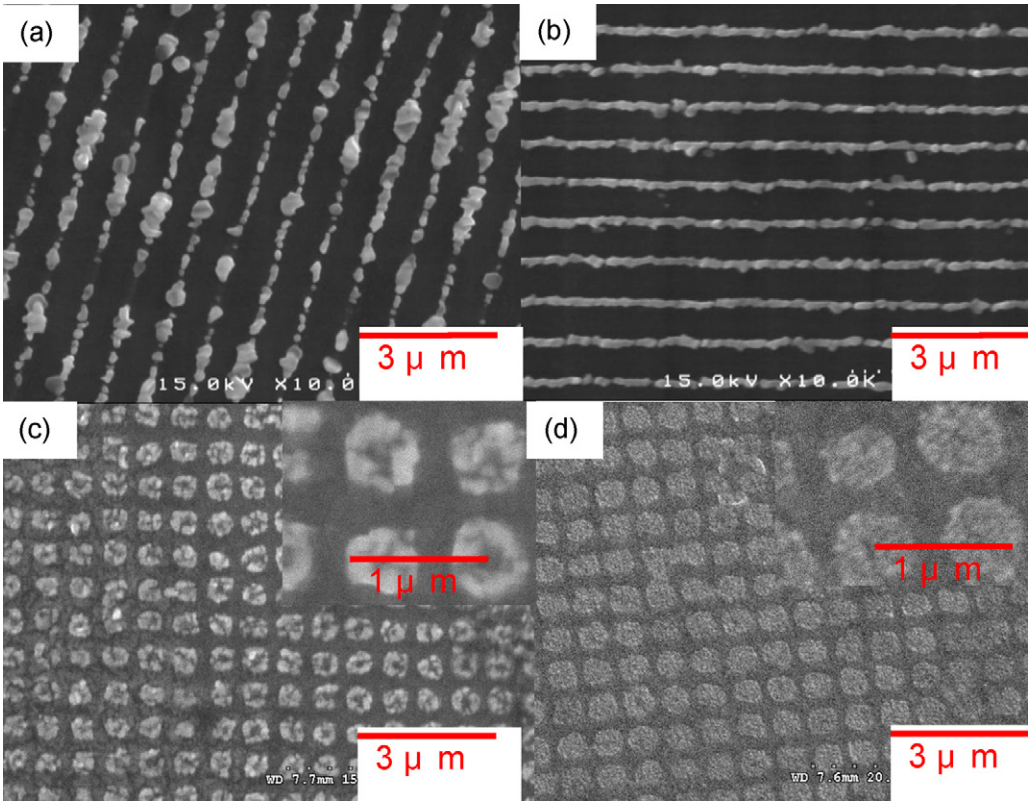

Fig. 1. SEM micrographs of the patterned Zn seeds fabricated with different electroplating current density of (a) 20, (b) 5, (c) 5 and (d) 1 mA/cm^2 for 1 min on the ITO glass. Inserts are the high magnification SEM micrographs.

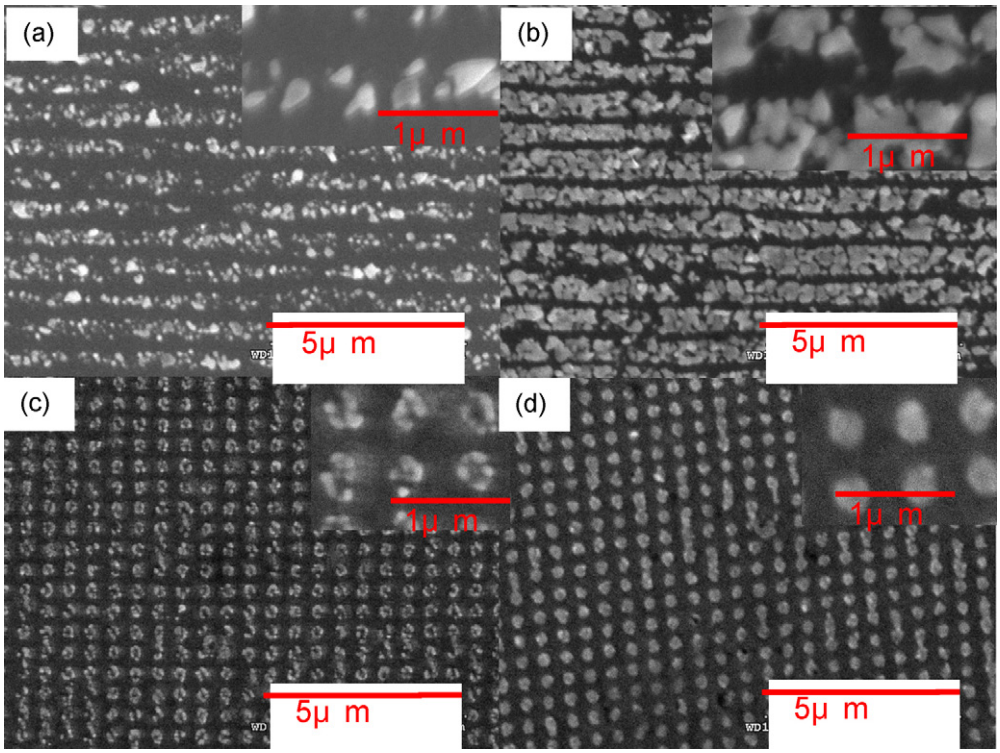

Fig. 2. SEM micrographs of the patterned Zn seeds fabricated for the reaction time of (a) 1 and (b) 3 min on the ITO glass. The current density of electroplating was 5 mA/cm^2. SEM micrographs of Zn nanopatterns were proceeded (c) without and (d) with annealing treatment at 300 °C for 30 min in air. Inserts are the high magnification SEM micrographs, respectively.

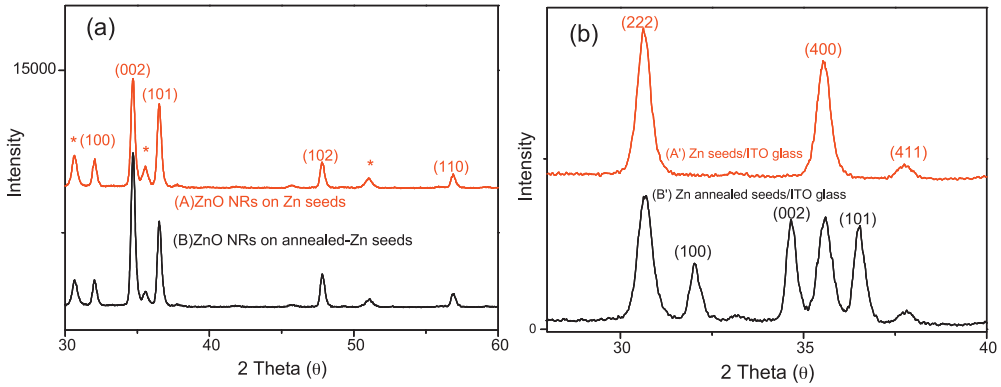

Fig. 3. (a) XRD patterns of ZnO nanorod arrays grown on (A) non-annealed and (B) annealed Zn-seeds on ITO glass substrate from 0.1 M $Zn(NO_3)_2{\cdot}6H_2O$ and HMT ($C_6H_{12}N_4$) aqueous solution at 90 °C for 3 h. (b) GIXRD patterns of (A′) Zn seeds/ITO glass and (B′) annealed Zn seeds/ITO glass. The symbol * indicates the reflection from the Zn-seeds on ITO glass substrate.

current density is too high, the lines will be more irregular, supposed to be due to the formation of pieces of zinc particles at large transient currents.

From Fig. 2, the deposition time has a great influence on the electroplated patterns of Zn seeds. Fig. 2(a) shows that when the electroplating time is too short, the zinc seeds will be incomplete on the sample of imprinted pattern on ITO substrate. Conversely, Fig. 2(b) has a completely transferred seeds on regions outside patterned PMMA on ITO substrate. The parameters of electroplating process are controlled properly that a complete pattern will be obtained. After the electroplating process of Zn seeds, the patterned substrate is heated at 300 °C (ITO/glass) for 30 min in air, as shown in Fig. 2 (c) and (d). Through this annealing process, the Zn seeds have partially transformed into ZnO nanoparticles (because the larger grains of the annealed samples as shown from the XRD data shown later) and those nanoparticles also can act as nucleation seeds for ZnO nanostructure growth.

Fig. 3(a) shows the XRD spectra of ZnO nanorods grown on electroplated Zn seeds/ITO glass substrate at 5 mA/cm^2 for 1 min. The diffraction peaks can be indexed to those all of hexagonal ZnO with polycrystalline structures on substrate. The intensity of the (0 0 2) diffraction is much stronger than other peaks, indicating that the ZnO nanorods have a preferred orientation along the [0 0 1] direction, especially in the ZnO NRs grown on annealed Zn seeds. The XRD pattern of Fig. 3(b) shows the Zn seeds/ITO glass (A′) and annealed Zn seeds/ITO glass (B′), respectively. However, the XRD pattern shows the polycrystalline nature of ZnO of Fig. 3(B′) and planes corresponding to (1 0 0), (0 0 2) and (1 0 1). We suggest that the preferred growth of ZnO NRs grown on annealed Zn seeds/ITO glass is due to the preferred orientation of the annealed seeds.

In Fig. 4, the schematic diagram is presented to describe the patterned growth of ZnO nanorods. It consists of four steps: (1) patterning of PMMA by solvent assist imprinting, (2) deposition of patterned Zn seeds by electroplating, (3) polymer stripping, and (4) ZnO nanorods grown on Zn seeds using the aqueous solution method. A simple strip pattern is imprinted on the ITO glass, followed by the preparation of Zn patterns using varied electroplating currents and precursor concentrations to study the effect of these conditions on the final dimensions of

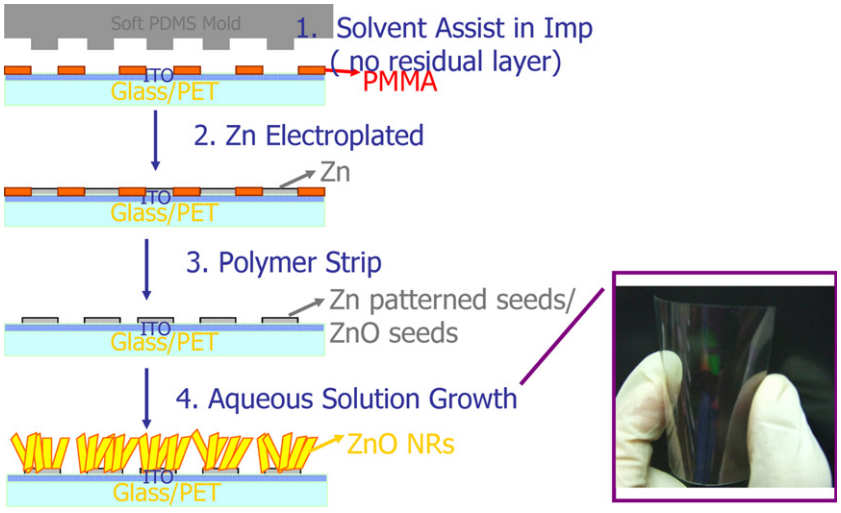

Fig. 4. Schematic diagram of the patterned growth of ZnO nanorods on the ITO substrate. Insert shows the optical images of the patterned Zn seeds on PET substrate by this technique.

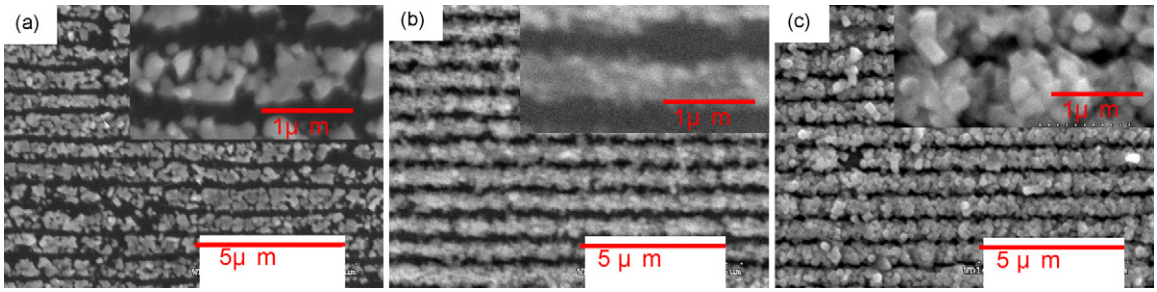

Fig. 5. SEM micrographs of patterned ZnO nanowire arrays with various concentration of $Zn(NO_3)_2$ and $C_6H_{12}N_4$. (a) Nanopattern of Zn seeds; and ZnO nanorods grown from in the reaction solution with concentration of (b) 0.025 M, and (c) 0.1 M, respectively. Inserts are the high magnification SEM micrographs.

the ZnO nanorods obtained. An optimized condition for the seeding process is selected for further experiments regarding the patterned growth of ZnO nanorods. The patterned zinc is then used as seeds to guide ZnO growth onto substrate. Insert in Fig. 4 shows the optical image of the patterned Zn seeds on PET substrate formed by this technique. The patterns are completely transferred from the PDMS mold to the substrate and the different colors represent different domains of the patterned seeds. In general, conventional nanoimprinting requires an additional oxygen plasma etching step to remove the residual polymer layer in the imprinted regions, which increases process time and complexity. Even though an ultrafast patterning method is available, there still remains the problem of the removal of a residual layer [16] [17]. However, the nanoimprinting method used in the present study is effective in proceeding without residual layer, which favors to get selective growth of Zn seeds and to obtain ZnO nanorods arrays in the subsequent steps. In other words, we have succeeded in the low temperature fabrication of Zn seeds to selectively grow patterned ZnO nanorods on transparent conductive substrate.

Nanoimpritng of the PMMA pattern without residual layer can facilitate the subsequent deposition of Zn seed layer by selective electroplating. The next step, ZnO nanorods grown on Zn seeds, uses aqueous solutions. When the patterned substrates are immersed into a precursor solution with lower concentration, the diameters of the as-synthesized nanorods decreased significantly. Fig. 5(b and c) shows the SEM images of nanorods synthesized on the selective positions after immersing in solution with equimolar precursor concentration of $Zn(NO_3)_2{\cdot}6H_2O$ and hexamethylenetetramine at 90 °C for 3 h. The as-synthesized nanorods have diameters in the range of 60–400 nm. The growth of much thicker ZnO nanorods is due to the increased precursor concentration. This growth phenomenon is similar to aligned growth of ZnO nanorods on blank substrates without patterns.

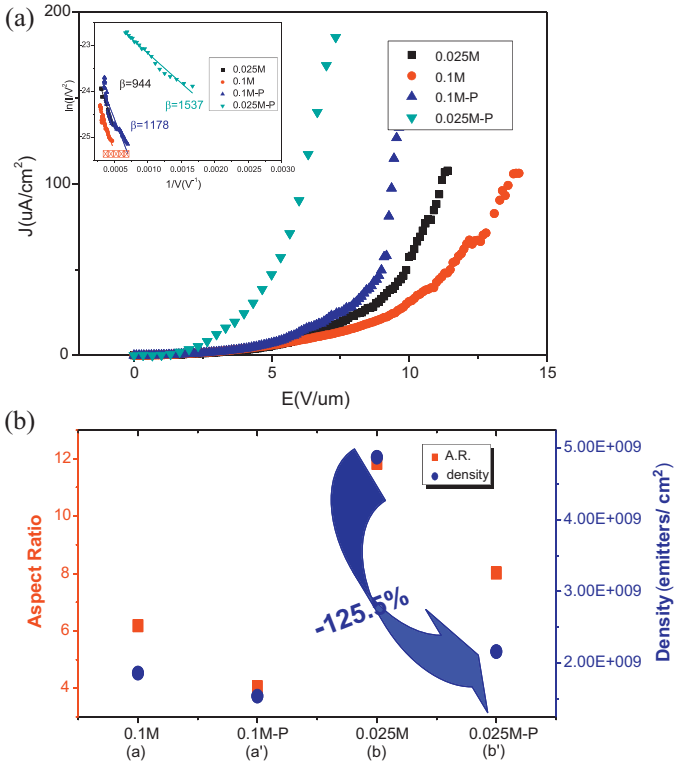

Fig. 6. (a) Field emission characteristics in J–E and $\ln(J/E^2)$–$1/E$ (inset) plots of the patterned and non-patterned ZnO field emitters. The straight line is a linear fit to the $\ln(J/E^2)$–$1/E$. (b) The diagram of aspect ratio and density of non-patterned and patterned ZnO NWs.

Fig. 6(a) gives the variation in the field emission performance in patterned and non-patterned ZnO field emitters. As shown in Fig. 6(a), the turn-on electric field is calculated to be 1.66 V/μm and 1.39 V/μm (at current density 0.1 μA/cm^2) for non-patterned ZnO nanorods using precursor concentrations of 0.1 and 0.025 M, respectively. The threshold field is 6.55 V/μm and 6.19 V/μm (at current density 10 μA/cm^2) for precursor concentrations of 0.1 and 0.025 M, respectively. However, after the patterned-growth process with 200 nm width Zn seeds, for 0.1 M and 0.025 M precursors, the turn-on electric field decreases to 0.28 V/μm and 0.97 V/μm, respectively. Therefore, the field emission characteristic of the ZnO cathode becomes much better emitter by patterned process.

The inset of Fig. 6 (a) is the corresponding Fowler–Nordheim (FN) plots, which shows that the field emission behaviors of the ZnO field emitters can be well described by the FN formula. The terms of the field enhancement factor (β) and work function (φ) can be analyzed from FN plots. Since a linear relation between $\ln(J/E^2)$ and $1/E$ is observed, the F–N formula is expressed as [18]

$$J = \frac{A\beta^2 E^2}{\varphi} \exp\left(\frac{-B\varphi^{3/2}}{\beta E}\right) \quad (1)$$

Table 1
The aspect ratio (A.R.), density, turn-on field and field enhancement factor (β) of the non-patterned ((a), (b)) and patterned ((a′), (b′)) ZnO NWs by various concentration.

Conc. of precursors of ZnO emitter	A.R.	Density (nanorods/cm^2)	Turn-on field (V/μm)		β
			0.1 μA/cm^2	10 μA/cm^2	
(a) 0.1 M	6.18	1.86×10^9	1.66	6.55	933
(b) 0.025 M	11.84	1.54×10^9	1.39	6.19	944
(a′) 0.1 M-P	4.05	4.87×10^9	1.38	5.63	1178
(b′) 0.025 M-P	8.02	2.16×10^9	0.42	2.44	1537

where J is the current density in mA/cm^2, E is the applied field strength in V/μm, A and B are constants being 1.56×10^{-6} A V^{-2} eV and 6.38×10^3 V eV$^{-3/2}$ μm^{-1}, respectively. The φ is the work function of the emitter that is related to the surface states, and β is the field enhancement factor that is introduced to reflect the degree of the field emission enhancement of any tip over a flat surface, i.e., β represents the true value of the electric field at the tip compared to its average macroscopic value. For nanostructured ZnO, the value of β is related to the geometry, crystal structure, and nanostructure density [19–21]. According to Eq. (1), the slope of FN plot can be obtained after plotting $\ln(J/E^2)$ versus $1/E$. From the FN plot, it is expected that the larger the slope, the higher the electric field factor (β). After patterning process, the slope is steeper and it means that enhancement factor is larger. Fig. 6(b) presents the aspect ratio and density of non-patterned ((a and b)) and patterned ((a′ and b′)) ZnO nanorods. After patterning process, the emitter density will decrease 1.25 times in precursor solution of 0.025 M and the estimated field enhancement factor β is 1537.

It can be clearly seen that the electric field listed in the Table 1 that (a) 0.1 M (6.55 V/μm) is higher than the (b) 0.025 M (6.19 V/μm). In addition, (b) 0.025 M (6.19 V/μm) is also significantly higher than (b′) 0.025 M-patterned (2.44 V/μm). These results indicate that the electric field is predominantly determined by the density of ZnO nanorods. Because the as-grown ZnO nanorods are dense enough to cause screen effect between ZnO nanorods, therefore, the highly efficient field emission of the patterned arrays can be attributed to the reduction of the screen effect. There are already many reports about the methods to diminish the screen effect of the ZnO nanorods [22–24]. After considering the cost and ease of operation of the technique, the patterned growth process described in this report is obviously an efficient method to control emitter density to diminish the screen effect and get a better FE performance.

4. Conclusion

In conclusion, the present work describes nanoimprinting and Zn electroplating to define seed pattern and to guide the selective growth of ZnO nanostructure through aqueous solution methodology at a low temperature of 90 °C. The structure analysis of the selectively grown ZnO nanorods shows that these structures are grown along the c-axis. The field emission from the ZnO nanorod arrays shows a high β value (high field enhancement factor) and low turn-on field. In this paper, we provide a way to fabricate high performance electron emitters in which the methodology is fast, more controllable, and less chemicals involved.

References

[1] J.B. Baxter, E.S. Aydil, Dye-sensitized solar cells based on semiconductor morphologies with ZnO nanowires, Solar Energy Mater. Solar Cells 90 (2006) 607–622.
[2] B.D. Yuhas, P. Yang, Nanowire-based all-oxide solar cells, J. Am. Chem. Soc. 131 (2009) 3756–3761.
[3] X.G. Han, H.Z. He, Q. Kuang, X. Zhou, X.H. Zhang, T. Xu, Z.X. Xie, L.S. Zheng, Controlling morphologies and tuning the related properties of nano/microstructured ZnO crystallites, J. Phys. Chem. C 113 (2009) 584–589.
[4] A. Umar, M.M. Rahman, Mohammad Vaseem, Y.B. Hahn, Biosensor based on low temperature grown ZnO nanoparticles, Electrochem. Commun. 11 (2009) 118–121.
[5] Dewei Chu, M. Yoshitake, O. Tatsuki, K. Kazumi, Formation and photocatalytic application of ZnO nanotubes using aqueous solution, Langmuir 26 (2010) 2811–2815.
[6] J.H. Jun, H.J. Seong, K. Cho, B.M. Moon, S. Kim, Ultraviolet photodetectors based on ZnO nanoparticles, Ceram. Int. 35 (2009) 2797–2801.
[7] H. Chen, Y. Liu, C.S. Xie, J. Wu, Dawen Zeng, Y. Liao, A comparative study on UV light activated porous TiO_2 and ZnO film sensors for gas sensing at room temperature, Ceram. Int. 38 (2012) 503–509.
[8] S. Noriko, H. Hajime, S. Takashi, O. Naoki, S. Isao, K. Kunihito, Low-temperature fabrication of light-emitting zinc oxide micropatterns using self-assembled monolayers, Adv. Mater. 14 (2002) 418–421.
[9] X.X. Zhang, D.F. Liu, L.H. Zhang, W.L. Li, M. Gao, W.J. Ma, Y. Ren, Q.S. Zeng, Z.Q. Niu, W.Y. Zhou, A.S. Zie, Synthesis of large-scale periodic ZnO nanorod arrays and its blue-shift of UV luminescence, J. Mater. Chem. 19 (2009) 962–969.
[10] X.D. Wang, C.J. Summers, Z.L. Wang, Large-scale hexagonal-patterned growth of aligned ZnO nanorods, Nano Lett. 4 (2004) 423–426.
[11] C.S. Liu, Y. Masuda, Z.W. Li, Q. Zhang, T. Li, Site-selective growth of highly oriented ZnO rod arrays on patterned functionalized Si substrates from aqueous solution, Cryst. Growth Des. 9 (2009) 2168–2172.
[12] Y.L. Tao, M. Fu, A.L. Zhao, D.W. He, Y.S. Wang, The effect of seed layer on morphology of ZnO nanorod arrays grown by hydrothermal method, J. Alloys Compd. 489 (2010) 99–102.
[13] Q. Ahsanulhaq, A. Umar, Y.B. Hahn, Growth of aligned ZnO nanorods and nanopencils on ZnO/Si in aqueous solution: growth mechanism and structural and optical properties, Nanotechnology 18 (2007) 115603 (7 pp.).
[14] Z.P. Zhang, H.D. Yu, Y.B. Wang, M.Y. Han, Aggregation-driven growth of well-oriented ZnO nanorod arrays, Nanotechnology 17 (2006) 2994–2997.
[15] Z.R. Tian, J.A. Voigt, J. Liu, B. Mckenzie, M.J. Mcdermott, M.A. Rodriguez, H. Konishi, H. Xu, Complex and oriented ZnO nanostructures, Nat. Mater. 2 (2003) 821–826.

[16] X. Cheng, L.J. Guo, One-step lithography for various size patterns with a hybrid mask-mold, Microelecon. Eng. 71 (2004) 288–293.
[17] K.L. Lai, I.C. Leu, M.H. Hon, Soft imprint lithography using swelling/deswelling characteristics of a polymer mold and a resist induced by a poor solvent, J. Micromech. Microeng. 19 (2009) 037001 (5 pp.).
[18] R.H. Fowler, L.W. Nordfeim, Electron emission in intense electric fields, Proc. R. Soc. A: Math. Phys. Eng. Sci. 119 (1928) 173–181.
[19] A. Wei, X.W. Sun, C.X. Xu, Z.L. Dong, M.B. Yu, W. Huang, Stable field emission from hydrothermally grown ZnO nanotubes, Appl. Phys. Lett. 88 (2006) 213102–213105.
[20] C.X. Xu, X.W. Sun, Field emission from zinc oxide nanopins, Appl. Phys. Lett. 83 (2003) 3806–3808.
[21] C.X. Xu, X.W. Sun, B.J. Chen, Field emission from gallium-doped zinc oxide nanofiber array, Appl. Phys. Lett. 84 (2004), 1540–1502.
[22] N.S. Liu, G.J. Fang, W. Zeng, H. Long, L.Y. Yuan, X.Z. Zhao, Diminish the screen effect in field emission via patterned and selective edge growth of ZnO nanorod arrays, Appl. Phys. Lett. 95 (2009) 153505–153507.
[23] J. Liu, J.C. She, S.Z. Deng, J. Chen, N.S. Xu, Ultrathin seed-layer for tuning density of ZnO nanowire arrays, J. Phys. Chem. C 112 (2008) 11685–11690.
[24] D. Cheyns, K. Vasseur, C. Rolin, J. Genoe, J. Poortmans, P. Heremans, Nanoimprinted semiconducting polymer films with 50 nm features, Nanotechnology 19 (2008) 424016–424021.